

# IMPACT RESPONSE ANALYSIS OF LARGE SCALE RC GIRDER WITH SAND CUSHION

Abdul Qadir BHATTI<sup>\*1</sup>, Norimitsu KISHI<sup>\*2</sup>, Shin-ya OKADA<sup>\*3</sup> and Hisashi KONNO<sup>\*4</sup>

## ABSTRACT

In order to establish a proper finite element model of prototype RC girder with sand cushion for impact response analysis, dynamic response analysis of RC girder with sand cushion subjected to falling weight impact force was performed to improve the state of the art of protective design for real scale rock-sheds by using LS-DYNA code. An applicability of proposed model was discussed comparing with experimental results (e.g. impact force, reaction force, and displacement waves). From this study, it is seen that the dynamic characteristics of impact response can be better simulated by using the proposed model.

**Keywords:** prototype RC girder, impact resistant design, sand cushion, impact response analysis, Drucker-Prager yield criterion

## 1. INTRODUCTION

In order to ensure the safety of rock-sheds, nuclear power plants, fuel tanks and/or other protective structures against impact loads, many numerical and experimental researches have been carried out [1]. A great deal of efforts have been made for the investigation on impact behavior and resistance of the structures when flying and/or falling bodies applied on the structures directly [2]. Otherwise, it will be one of engineering approaches to attenuate the impact forces by using absorbing system. Rock falls are one of the most prevailing natural hazards in the mountainous regions. Rock-sheds are used to protect lives and lifelines against these potential rock impacts. Cushion materials are laid on the roof of rock-sheds to absorb the rock fall impact energy, which is one of the main input parameters in design of the rock shed and, still now these structures have been designed based on an allowable stress design concept using simply estimated maximum impact force [3]. However, in order to rationally design this type RC structures considering the performance up to ultimate state, impact resistant behavior and dynamic load-carrying for these should be investigated precisely. For these, not only experimental study but also numerical one should be performed.

From this point of view, here, in order to establish a rational numerical analysis method for real RC rock-sheds, nonlinear finite element analysis was conducted based on the falling weight impact

test results for prototype rectangular RC girder with partially mounted sand-cushion. An explicit and three dimensional finite element code LS-DYNA is used for this study [4].

## 2. OVERVIEW OF LARGE SCALE FALLING WEIGHT IMPACT TEST

### 2.1 Outline of testing model

RC girder, which is modeled for roof of real RC rock-sheds, is taken for falling-weight impact test of prototype RC structures. The girder is of rectangular cross section and the dimensions are of  $1.0 \times 0.85$  m and clear span is 8 m long. The dimensions of the sand cushion set on the center of girder are of  $1.5 \times 1.5 \times 0.9$  m. Fig. 1 shows dimensions of the RC girder, arrangement of rebars, and measuring points for each response wave. In this figure, it is confirmed that 7#D29 rebars are arranged which is for 0.64 % of main rebar ratio corresponding to designing of real RC rock-sheds and 4#D29 rebars are arranged as the upper axial rebar in which the rebar volume corresponds to a half of main rebar ratio. Axial rebars were welded to 12 mm steel-plate at the ends for saving of anchoring length of the rebars. Thickness of concrete cover is assumed to be 150 mm as well as real rock-sheds. D13 stirrups are arranged with intervals of 250 mm which is less than a half of an effective height of the cross section. In this study, arranging interlayer stirrups and upgrading in shear load-carrying capacity, the RC girder was designed to be failed with flexu-

\*1 Graduate Student, Muroran Institute of Technology Japan, M.E., JCI Member

\*2 Prof., Dept. of Civil Engineering, Muroran Institute of Technology Japan, Dr.E., JCI Member

\*3 Researcher, Civil Engineering Research Institute (CERI) for cold region, M.E., JCI Member

\*4 Senior Researcher, Civil Engineering Research Institute (CERI) for cold region, Dr.E., JCI Member

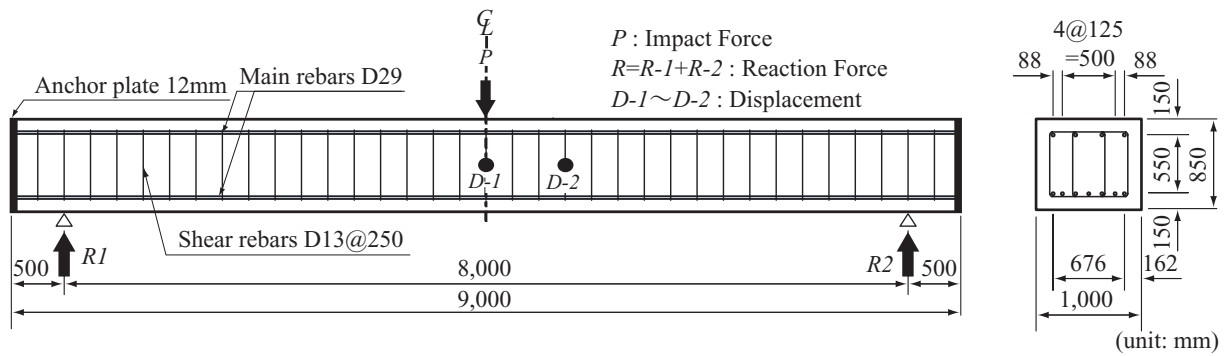


Fig. 1 Dimensions of RC girder and measuring items

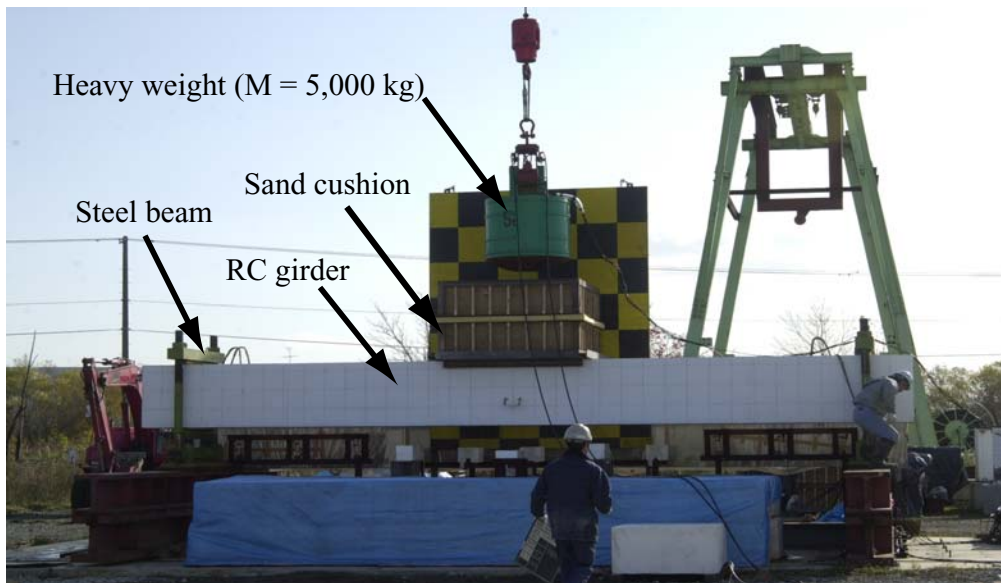


Photo 1 Pictorial view of the experimental setup with falling height of 10 m

ral failure mode. The detailed static design parameters of the RC girder are listed in Table 1. Static flexural and shear load-carrying capacities  $P_{usc}$  and  $V_{usc}$  were calculated based on Japanese Concrete Standards [5]. From this table, it is confirmed that the RC girder designed here will fail with flexural failure mode under static loading. The static material properties of concrete and rebars during experiment are listed in Table 2.

## 2.2 Experimental method

In the experiment, 5,000 kg heavy weight was lifted up to the prescribed height of 10 m by using the track crane, and then dropped freely to the mid-span of girder due to a desorption device. A heavy weight is made from steel outer shell with 1 m in the diameter, 97 cm in height, and spherical bottom with 80 cm in radius and its mass is adjusted filling concrete and steel balls.

RC girder was set on the supporting girders with load cells for measuring reaction force which are made so as to freely rotate but not to move toward each other. The ends of RC girder are fixed in

the upward direction using steel rods and beams to prevent from jumping up at the time of impacted by a heavy weight. In this experiment, impact force wave ( $P$ ), reaction force wave ( $R$ ), and displacement waves ( $D$ ) at six points along the girder were measured. Impact force wave was estimated using a deceleration of heavy weight, which is measured using accelerometers set at the top-surface of the weight.

The accelerometer is of strain gauge type and its capacity and frequency range for measuring are 1,000 times gravity and DC through 7 kHz, respectively. Each loadcell for measuring reaction force are of 1,500 kN capacity and more than 1 kHz measuring frequency. For measuring displacements, laser-type variable displacement transducers (LVDTs) were used which are of a 200 mm maximum stroke and 915 Hz measuring frequency. Those measured waves will be described later accompanying with the analytical results. After experiment, pictures for views of cracks occurred around impacted area and on side surface of RC girder, and a view of peeling and spalling of con-

Table 1 Static design parameters of RC girder

Shear rebar ratio $\rho_t$	Static shear depth ratio $a/d$	Static shear capacity $V_{usc}$ (kN)	Static bending capacity $P_{usc}$ (kN)	Shear-bending capacity ratio $\alpha$
0.0064	5.71	1,794	619.8	2.894

Table 2 Material properties of concrete and rebar

Type	Density $\rho$ (ton/m <sup>3</sup> )	Elastic coefficient $E$ (GPa)	Poisson's ratio $\nu$	Yielding strength (MPa)
Concrete	2.343	25.4	0.177	31.2
Rebar D13	7.85	206	0.3	390
Rebar D29				400

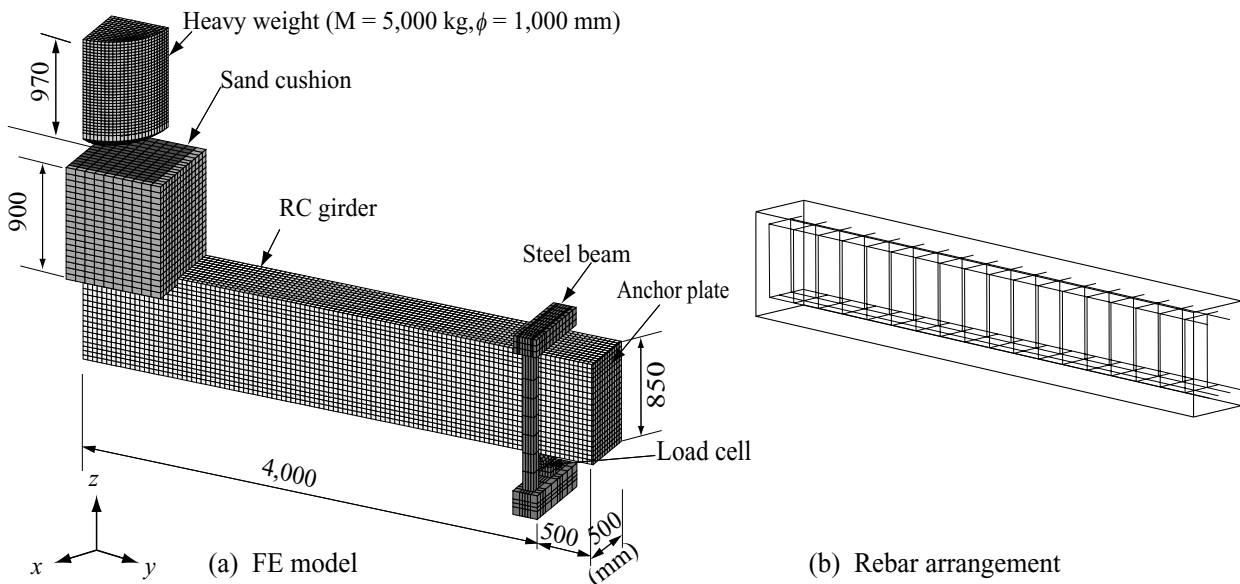


Fig. 2 Finite element mesh scheme for RC girder

crete cover were taken. Those cracks were also sketched and the crack patterns will be discussed latter by comparing with the analytical ones.

Photo 1 shows experimental setup of falling-weight impact test for RC girder partially mounted with sand cushion.

### 3. ANALYTICAL OVERVIEW

#### 3.1 Finite Element model

One quarter of RC girder was three-dimensionally modeled for numerical analysis with respect to the two symmetrical axes. Four side-surfaces of sand cushion were confined laterally. Fig. 2(a) shows a mesh geometry of the girder with sand as absorbing material. A geometrical configuration of the heavy weight and sand cushion were

precisely modeled following the real ones.

Supporting giggers including loadcells and the gigue for protecting the girder from jumping up were also precisely modeled corresponding to the real ones. In this model, axial rebar and stirrup were modeled using beam element having equivalent axial stiffness, cross sectional area and mass with those of real ones. The others were modeled using eight-node and/or six-node solid elements. The mesh geometries for axial rebar and stirrup arrangement are shown in Fig. 2(b). Number of integration points for solid and beam elements are one and four, respectively.

Total number of nodal points and elements for one-fourth model are of 43,838 and 38,167, respectively. In order to take into account of contact interface between sand and a head of heavy

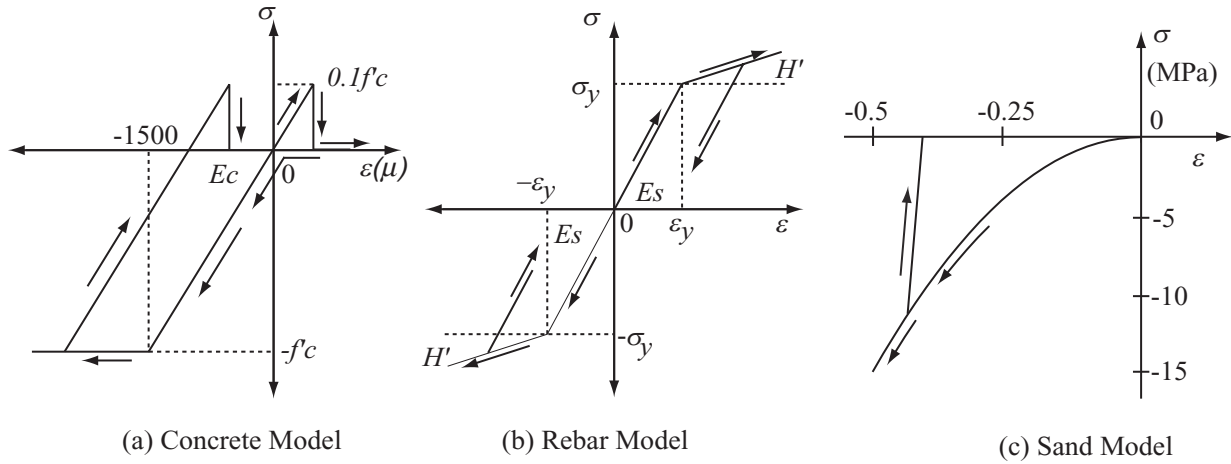


Fig. 3 Stress-strain relation of material constitutive models

weight elements and between adjoining concrete and supporting gigue elements, contact surface elements for those are defined, in which contact force can be estimated by applying penalty methods for those elements but friction between two contact elements was not considered. In applying this penalty method, each slave node is checked for penetration through the master surface. If the slave node does not penetrate, nothing is done. If it does penetrate, an interface force is applied between the slave node and its contact point. The magnitude of this restoring force is proportional to the penetration distance into the solid and acts in the normal direction to the surface of the solid. A head of heavy weight was set so as to contact with the impacting point of the upper surface of sand cushion mounted at the mid span of RC girder and predetermined impact velocity was applied to all nodal points of the heavy weight model.

### 3.2 Modeling of materials

Fig. 3 shows the stress and strain relations for each material: concrete; rebar; and sand. Neither strain rate effects of concrete and rebar nor softening phenomena of concrete were considered for this elasto-plastic impact response analysis method for the RC girder. But viscous damping factor of  $h = 0.2\%$  was considered which is proportional to mass of RC girder. The constitutive laws for each material characteristic are briefly described as below:

#### (1) Concrete

Stress-strain relationships of concrete was assumed by using a bilinear model in compression side and a cut-off model in tension side as shown in Fig. 3(a). It is assumed that 1) yield stress is equivalent to compressive stress  $f'_c$ ; 2) concrete yields at 0.0015 strains; 3) the tensile stress is perfectly released when an applied pressure reaches tensile strength of concrete; 4) the tensile strength is set to be  $1/10^{th}$  of the compressive strength; and 5) von Mises criterion was applied to the yielding of con-

crete.

#### (2) Rebar

For main rebars and stirrups, an elasto-plastic model following isotropic hardening rule was applied as shown in Fig. 3(b). Here, the plastic hardening modulus  $H'$  was assumed as 1% of elastic modulus  $E_s$  ( $E_s$ : Young's modulus). The yielding condition was judged based on von Mises criterion.

#### (3) Sand cushion

Fig. 3(c) shows the constitutive model for sand cushion. To rationally analyze in stress behavior of sand cushion when a heavy weight collides, second order parabolic stress-strain relation for sand cushion [3] was applied in which the constitutive relation is described in the following expression.

$$\sigma = 50\varepsilon^2 \quad (1)$$

Here,  $\sigma$  is stress and  $\varepsilon$  is the volumetric strain. Here, referring to reference [3], material properties of sand for impact response analysis were assumed as; Young's modulus  $E_{sand} = 10$  GPa; Poisson's ratio  $\nu_{sand} = 0.06$ ; and density  $\rho_{sand} = 1,600$  kg/m<sup>3</sup>.

#### (4) Falling weight, support treatment device, and anchor plate

The other elements (steel weight, supporting apparatus and anchor plate) were modeled as elastic body based on experimental observations.

Young's modulus, Poisson's ratio and density were assumed as  $E = 206$  GPa,  $\nu_s = 0.3$ , and  $\rho_s = 7.85 \times 10^3$  kg/m<sup>3</sup>, respectively.

## 4. COMPARISON BETWEEN ANALYTICAL AND EXPERIMENTAL RESULTLS

### 4.1 Time histories of impact force, reaction force, and displacement

Fig. 4 shows the comparisons between the impact response waves of the girder obtained using

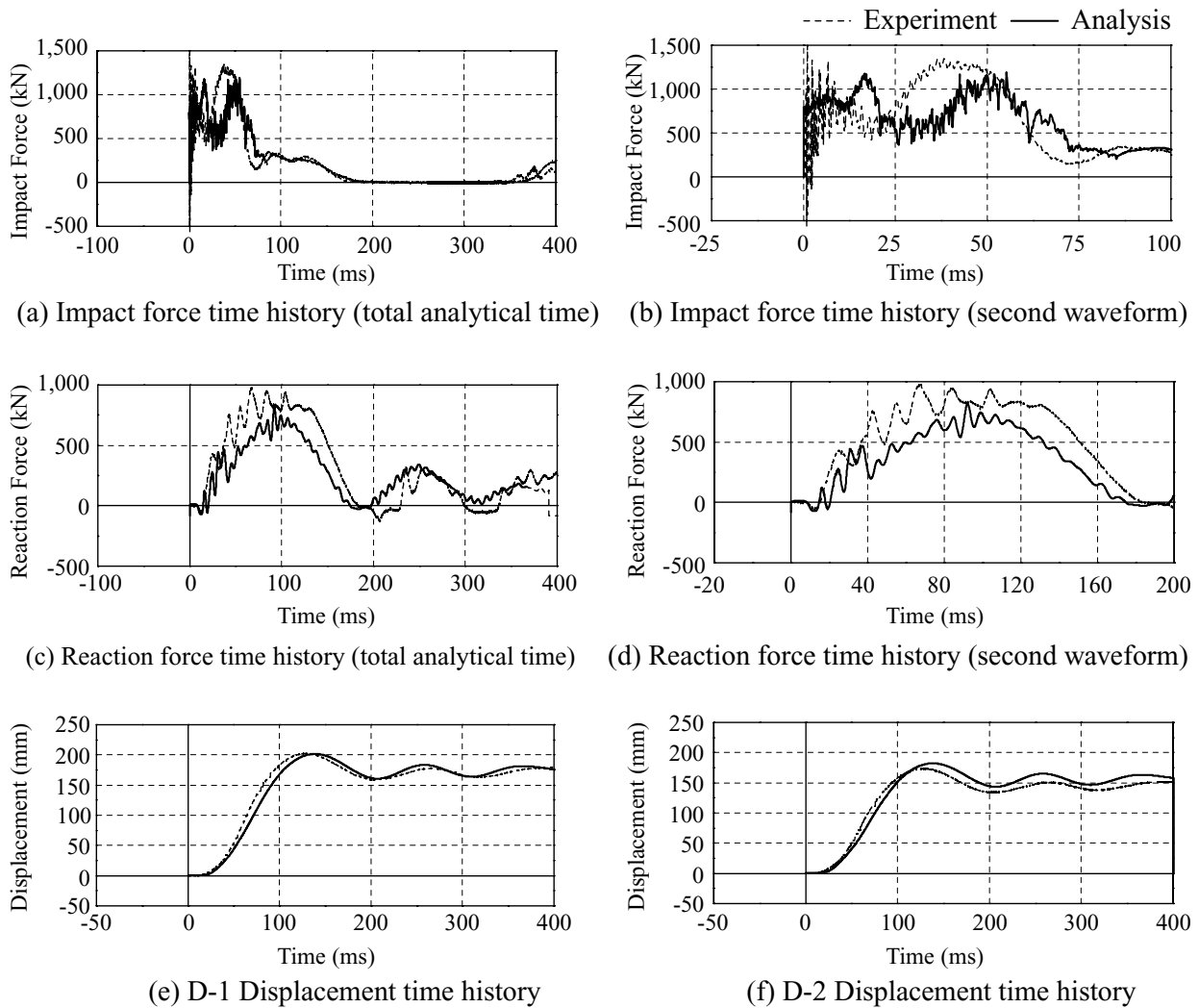


Fig. 4 Comparison between analytical and experimental results

finite element analysis method with the experimental results. For each response wave, characteristics of wave and an applicability of proposed numerical analysis method comparing with experimental results will be discussed below.

Figs. 4(a) and 4(b) show the time histories of impact force waves during 400 ms and 100 ms, respectively. From those figures, it is observed that; 1) duration time of impact force wave is roughly 180 ms; 2) the wave is mainly composed of a damped sinusoidal wave and three waves with gradually elapsed period; 3) the wave during about 75 ms from the beginning of impact may be excited due to interacting between heavy weight and having compacted sand, and the wave after that may be occurred due to both heavy-weight and compacted sand impacting against the RC girder; and 4) during about 25 ms at beginning of impact, high frequency and high amplitude waves are also excited. However, the high frequency and high amplitude wave may be come out from vibration characteristics of accelerometer and/or stress wave transmitted in the

weight, because the high frequency wave components are hardly excited in the heavy-weight due to colliding against sand which is of extremely loose and soft comparing with the weight. By comparing the results obtained from analytical and experimental waves, it is confirmed that 1) duration time of a whole wave and wave configuration after about 75 ms from the beginning are in good correspondence with the experimental results; 2) period and phase of waves around the beginning of impact are a little different from the experimental results; but 3) the maximum response value may be almost same to each other.

From Figs. 4(c) and 4(d), for reaction force wave it is observed from experimental results that: 1) the loading time due to heavy weight is about 200 ms and 2) after unloading, the RC girder freely vibrates with damping having a period of 100 ~ 110 ms. Comparing with the analytical and experimental results, it is seen that the wave configurations from both results are almost same to each other, even though maximum amplitude from experimen-



Fig. 5 Experimental crack patterns on front side of RC girder



Fig. 6 Analytical crack patterns on front side of RC girder (white  $\leq 0.001$  MPa, dark/black  $> 0.001$  MPa)

tal results is a little bigger than that from analytical ones.

From Figs. 4(e) and 4(f) for displacement waves at the points D-1/2, it is confirmed that numerical response waves during the impact load surcharging to the RC girder are similar to those of the experimental results.

From Fig. 4(f), it is observed that numerically estimated period for free vibration is almost the same with that of experimental results and is about 100 ms. The maximum displacement obtained from numerical and experimental results is likely to be shown in Fig. 4 (e).

#### 4.2 Crack patterns on side-surface of RC girder

The crack pattern is predicted based on the principle that concrete stress is converted to zero when the pressure applied to an element reaches a tension cut-off value following the constitutive law of concrete assumed before.

The crack patterns obtained from experiments were sketched in black solid lines as shown in Fig. 5. Fig. 6 shows the contours of the maximum principal stress range from -0.001 to 0.001 MPa on the side-surface under the maximum displacement. The white colored elements can be considered as being cracked region. Fig. 6 shows that a series of white elements developed from the upper to the lower edge of the beam. Then, it is seen that the distribution of white colored elements are almost similar with the crack patterns obtained from experimental results. It is confirmed that the crack patterns observed experimentally can be predicted by using the proposed finite element analysis method.

### 5. CONCLUSIONS

In order to establish a proper finite element method of RC girder with prototype sand element for impact response analysis, dynamic response analysis of RC girder with sand cushion subjected

to falling weight impact force was conducted. An applicability of the proposed finite element method was discussed by comparing with the prototype experimental results. The results obtained from this study are as follows:

- (1) The response characteristics obtained using proposed numerical analysis have comparatively similar tendency for impact force ( $P$ ), reaction force ( $R$ ) and displacement ( $D$ ) wave form to those of experimental results;
- (2) The numerical analysis results obtained from impact force and reaction force time histories have a tendency to be smaller than that from experimental ones;
- (3) The displacement wave obtained from numerical analysis corresponds to the experimental results well; and
- (4) Crack patterns of concrete on side-surface can be roughly predicted using the proposed finite element method.

### ACKNOWLEDGEMENT

The authors gratefully acknowledge the support from Ministry of Education, Sciences and Culture (MEXT) in the form of research grant under the Monbukagakusho scholarship and also experimental support from Civil Engineering Research Institute (CERI) for cold regions.

### REFERENCES

- [1] Kishi, N., Mikami, H., Matsuoka, K.G., and Ando, T. (1999). "Elasto plastic impact behavior analysis of flexural failure type RC beam" *Journal of Structural Mechanics and Earthquake Engineering*, JSCE, 619(47), 215-233, (in Japanese).
- [2] Kishi, N., Mikami, H., Matsuoka, K.G., and Ando, T. (2002). "Impact behavior of shear-failure-type RC beams without shear rebar" *International Journal of Impact Engineering*, 27, 955-968.
- [3] Kishi, N., Okada, S., Konno, H., and Ikeda, K. (2003). "Numerical study on modeling of sand element for impact response analysis" *Journal of Structural Engineering*, JSCE, 49A, 1323-1332, (in Japanese)
- [4] Hallquist, J.O. (2000). "LS-DYNA User's Manual" Livermore Software Technology Corporation.
- [5] Japan Society of Civil Engineers (1996). "Standard Specifications for Concrete Structures in Japan" JSCE, (in Japanese).